A Deterministic Round Earth Loss Model for Open-Sea Radio Propagation

Kun Yang*, Andreas F. Molisch†, *Fellow, IEEE*, Torbjörn Ekman*, and Terje Røste*
*Department of Electronics and Telecommunications
Norwegian University of Science and Technology, NO-7491 Trondheim, Norway
Email: {kuny, torbjorn.ekman, terje.roste}@iet.ntnu.no
†Wireless Devices and Systems Group, Department of Electrical Engineering
Viterbi School of Engineering, University of Southern California, Los Angeles, California, 90089
Email:molisch@usc.edu

***Abstract*—This paper proposes a deterministic path-loss model for the open-sea environment. The model accounts for different effects including effective reflection, divergence, and diffraction due to rough sea and earth curvature. The model results show excellent agreement with experimental results from our recent measurement campaign, which investigated propagation at 2 GHz with a maximum distance of 45 km. Channel parameters like mean-square surface slope and standard deviation of surface height are evaluated, from which it can be concluded that the shadowing and scattering effects on the reflection ray will influence the fading amplitude within the distance of 0.6 First Fresnel Zone clearance.**

I. Introduction

Most maritime activities, such as shipping and fishing, happen within an exclusive economic zone (EEZ) of a country, which is defined as an area extending to a distance of 200 nautical miles from its costal baseline. Therefore, a broadband communication system which can cover the EEZ with high data rate and low cost will be more attractive than the current maritime communication systems like VHF and satellite systems. However, neither new system designs nor modifications of the current systems can be done without a comprehensive path loss model. For this reason, a number of path loss models have been previously proposed in the literature, but they all suffer from various sources of inaccuracies and inapplicabilities to EEZ-type distances.

In previous investigations, several deterministic models such as the Free Space Loss (FSL) model and the Plain Earth Loss (PEL) model based on Friis transmission formula and two-ray tracing method, respectively [3], have been commonly used as a reference for the open-sea environment [1],[2]. However, the earth curvature and sea roughness, which can not be ignored within the EEZ, have not been taken into account in the PEL model, leading to significant inaccuracies. The ITU-R Recommendation P.1546-2 [4] offers a method for point-to-area predictions of field strength for the maritime mobile services in the frequency range 30 MHz to 3000 MHz, and for distances in the range 1 km to 1000 km, being intended for radio planning. However, the fading dips, which occur at short TX-RX distances, are not included. Subsequently, a quasi-deterministic path-loss model was proposed by combining the PEL and ITU-R model in [5] to deal with both of the above-mentioned limitations. However, the scattering, divergence and shadowing effects still have not been taken into consideration in the PEL part. The current paper aims to fill this gap and provide a comprehensive and accurate channel model for the EEZ.

The rest of the paper is organized as follows: In section II the geometrical model with earth curvature is described briefly. In section III propagation phenomena like effective reflection from rough sea surface, divergence effect, diffraction effect for both the LOS and the reflection ray are presented in detail. Section IV is devoted to the REL model and evaluations of channel parameters including polarization, mean-square surface slope and standard deviation of surface height. Finally, conclusions are drawn in section V.

II. Geometrical model

While the classical PEL model is widely used for cellular communications [6], for distances beyond several kilometers, the earth can not be considered as a ‘plane’ earth. Therefore, a round earth geometrical model based on the two-ray method is used instead as shown in Fig. 1, where h_1 and h_2 are the TX and RX antenna height, respectively. The radius of earth ($\sim$ 6371 km) is denoted by r_e and d is defined as the RX-TX distance. According to the two-ray method and with the reference to Fig 1, the received signal level (RSL) P_RX is obtained as:

$$\frac{P_\mathrm{RX}}{P_\mathrm{TX}} = \left(\frac{\lambda}{4\pi D_\mathrm{LOS}}\right)^2 \left|1 + R \cdot exp(jkD_\mathrm{diff})\right|^2 \tag{1}$$

Here, D_LOS represents the path length of the LOS, D_diff is the path length difference between the LOS and sea reflection expressed in equation (2), and R is the reflection coefficient from sea surface.

$$\begin{aligned} D_\mathrm{diff} &= X_1 + X_1 - D_\mathrm{LOS} \quad (2)\\ d &= D_1 + D_2 \quad (3)\end{aligned}$$

where

$$\begin{aligned} D_\mathrm{LOS} &= \sqrt{(r_\mathrm{e}+h_1)^2 + (r_\mathrm{e}+h_2)^2 - \xi} \quad (4)\\ \xi &= 2(r_\mathrm{e}+h_1)(r_\mathrm{e}+h_2)\cos\left(\frac{d}{r_\mathrm{e}}\right) \quad (5)\end{aligned}$$

The X_1 and X_2 can be obtained as

$$\begin{aligned} {X_1}^2 &= (h_1 + r_e)^2 + {r_e}^2 - 2(r_e + h_1) r_e \cos\alpha & (6) \\ {X_2}^2 &= (h_2 + r_e)^2 + {r_e}^2 - 2(r_e + h_2) r_e \cos\beta & (7) \end{aligned}$$

and α and β can be calculated by:

$$\begin{aligned} &\arccos\left(\frac{r_e + h_1 - r_e cos\alpha}{X_1}\right) + \alpha = ... \\ &\qquad \arccos\left(\frac{r_e + h_2 - r_e cos\beta}{X_2}\right) + \beta \qquad (8) \end{aligned}$$

$$\alpha + \beta = \frac{d}{r_e} \qquad (9)$$

However, the round earth geometrical model only takes the sea reflection into consideration, based on the two-ray method. It is insufficient because the earth curvature will gradually shadow both the LOS and sea reflection when the TX-RX distance increases. In addition, divergence on the reflection path from the spherical earth curvature needs to be taken into account. Last but not least, the effective reflection coefficient from the rough sea surface is also different from that of idealized specular reflections. Summarizing the following effects based on two-ray method need to be accounted for:

$$\begin{cases} \text{LOS} \begin{cases} \text{Free space Loss} \\ \text{Diffraction Loss} \end{cases} \\ \\ \text{Sea Reflection} \begin{cases} \text{Effective Reflection} \\ \text{Divergence} \\ \text{Shadowing Effect} \\ \text{Diffraction Loss} \end{cases} \end{cases} \qquad (10)$$

All these effects will be described in the Section III in detail.

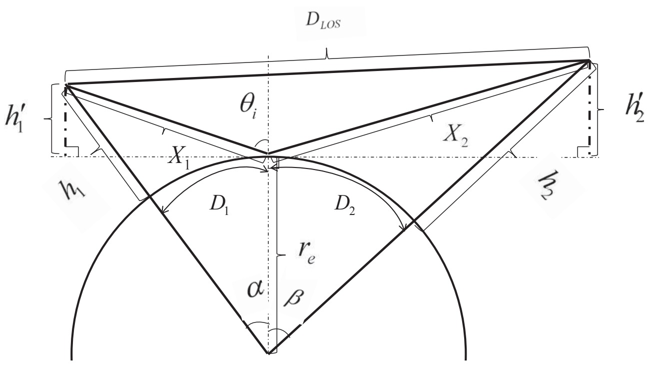

Fig. 1. Geometrical model for the REL model.

III. Propagation phenomena

A. Effective reflection from roughness surface

Specular reflection theory is based on a assumption that the reflection surface is smooth. However, the sea surface is seldom smooth due to the roughness caused by sea movement, which will make the specular reflection model unsuitable for mobile radio frequencies, especially for big-wave surfaces occurring during bad weather conditions. The roughness of the sea surface will result in a power reduction of the specular reflected ray, because part of the reflected power will be scattered in other directions, as shown in Fig. 2(a). Two main theories have been proposed for scattering by rough surfaces: the Kirchhoff theory and the perturbation theory [6]. The Kirchhoff theory assumes that any point on the surface doesn't shadow other points of the surface. In addition, the height distribution of the surface is assumed to follow a Gaussian distribution, which is the case for rough sea waves [7]. Under these assumptions, the effective reflection coefficient R_{rough} becomes:

$$R_{\text{rough}} = R \cdot exp[-2 \left(\frac{2\pi\sigma_h sin\theta_e}{\lambda}\right)^2] \qquad (11)$$

where

$$\begin{aligned} h'_1 &= h_1 - 0.5 r_e \alpha^2 & (12) \\ h'_2 &= h_2 - 0.5 r_e \beta^2 & (13) \\ \theta_e &= \arcsin\left(\frac{h'_1}{X_1}\right) = \frac{\pi}{2} - \theta_i & (14) \end{aligned}$$

where σ_h is defined as the standard deviation of surface height distribution. θ_i and θ_e represent the incident angle and the elevation angle (for grazing angle, $\theta_e \approx 0$), respectively. R is the specular reflection coefficient. Under these assumptions, the effective reflection coefficient is smaller than the specular reflection coefficient and it decreases with increasing wave height standard derivation.

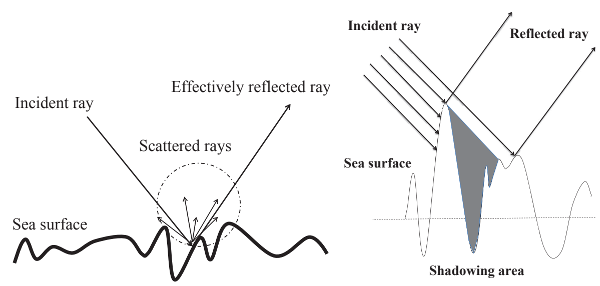

(a) Effective reflection by a rough sea surface.

(b) Shadowing effect.

Fig. 2. Effective reflection and Shadowing effect

B. Shadowing effect for the reflected ray

Equation (11) assumes that one point of the surface doesn't shadow other points of the surface. However, the sea surface may shadow other points on the surface (shown in Fig. 2(b)) when the elevation of the incident ray is small. This has been taken into consideration by Smith [9] by introducing a shadowing coefficient S_{fun}:

$$S_{\text{fun}} = \frac{1 - 0.5\text{erfc}\left(\frac{\tan\theta_i}{\sqrt{2}\beta_0}\right)}{\Lambda(\tan\theta_i) + 1} \qquad (15)$$

where

$$\Lambda(\tan\theta_i) = \frac{1}{2}\left(\sqrt{\frac{2}{\pi}}\frac{\beta_0}{\tan\theta_i}\exp^{-\frac{\tan\theta_i^2}{2\beta_0^2}} - \text{erfc}\left(\frac{\tan\theta_i}{\sqrt{2}\beta_0}\right)\right) \qquad (16)$$

where ${\beta_0}^2$ represents the mean-square surface slope, and the erfc is the error function complement. The measured rms surface slope β_0 can be found in [10], where it can be seen that the rms surface slope is generally found within [0.04, 0.07]. The shadowing effect is introduced by multiplying S_{fun} with the effective coefficient R_{rough}. The shadowing coefficient with different rms surface slope β_0 ($h_1 = 14.1\ \mathrm{m}, h_2 = 9.5\ \mathrm{m}$) is displayed in Fig. 3, where it can be seen that larger β_0 results in smaller S_{fun} at same TX-RX distance and the reflected ray will be totally shadowed beyond the distance D_0 (24.4 km for $h_1 = 14.1\ \mathrm{m}, h_2 = 9.5\ \mathrm{m}$), which is defined as the distance when LOS tangents the surface of the earth.

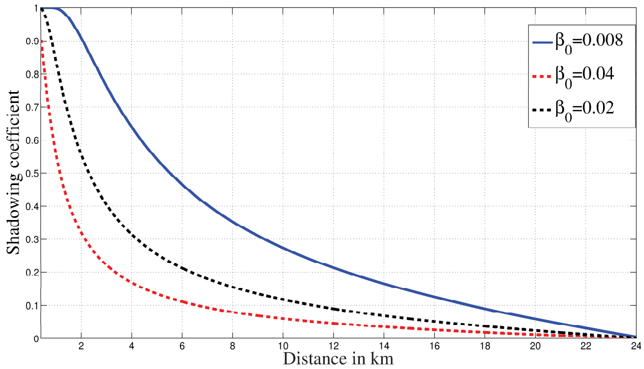

Fig. 3. Shadowing coefficient with different rms surface slope as a function of distance.

C. Divergence effect

The incident rays carry different amounts of power density from the reflected ray due to the earth curvature, which is defined as divergence effect and demonstrated in Fig. 4. The received signal level will decrease due to the decrease of power density caused by earth curvature. As a result, the effective reflection coefficient R_{rough} needs to be modified by multiplying it with a divergence coefficient D expressed by [8]:

$$D = \begin{cases} \dfrac{1}{\sqrt{1+\frac{2D_1D_2}{r_e(h_1'+h_2')}}} & \text{if } h_1' > 0, h_2' > 0 \\ 0 & \text{otherwise} \end{cases} \tag{17}$$

where h_1' and h_2' are the effective TX and RX antenna height (see equation (12-13)), respectively. D_1 and D_2 are in Fig. 1.

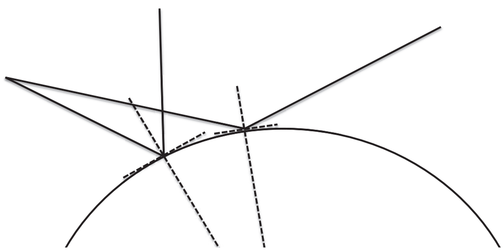

Fig. 4. Divergence effect.

The divergence coefficient D shown in Fig. 5 is obtained according to equation (17) by setting $h_1 = 14.1\ \mathrm{m}, h_2 = 9.5\ \mathrm{m}$, where it can be found that the divergence factor decreases with an increase of distance. As a result, the power of the reflected ray will decay to zeros (shown in Fig. 5 when a TX-RX distance is more than D_0).

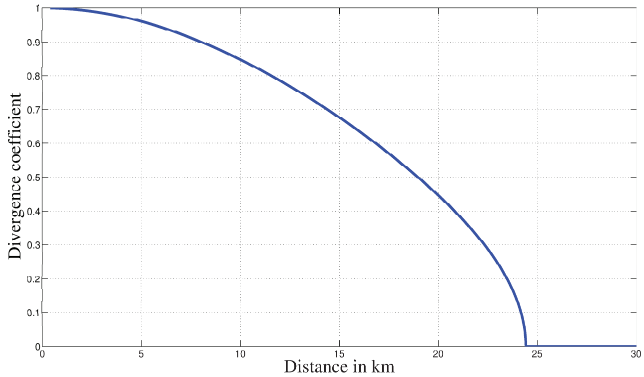

Fig. 5. Divergence factor as a function of distance.

D. Diffraction loss

The earth curvature will not only block the reflected ray but also the LOS. However, the diffraction effect will allow the radio transmission to continue even beyond the LOS, though suffering from a diffraction loss. Several papers [11][12] show the theory of ground-wave propagation over a smooth spherical earth, which fits the geometrical environments of the open-sea. Referring to [12], the total TX-RX distance d is divided into three parts d_1, d_2, d_3, which is given by using equation (18) and shown in Fig. 6.

$$d = d_1 + d_2 + d_3 \tag{18}$$

where d_1 and d_2 are the distances to the horizon which can be calculated by using:

$$d_n = \sqrt{2k_e r_e h_n} \qquad \text{n=1,2} \tag{19}$$

Here, k_e is the ratio of the effective earth's radius and true earth's radius, and h_1, h_2 are the antenna heights as displayed in Fig. 6.

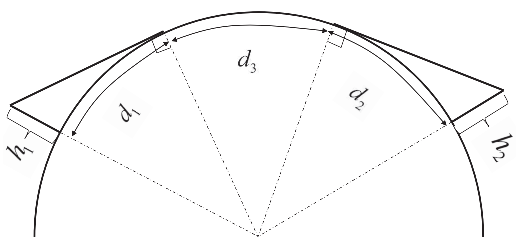

Fig. 6. Radio link beyond LOS over a smooth earth.

Each part will cause a corresponding loss $L_n, n = 1, 2, 3$, which is defined to be negative here, since it reduces the total RSL. The decibel loss L_1 and L_2 are obtained by using:

$$L_1 = 20\log_{10}\frac{N_1}{\sqrt{5.656\pi\zeta_1}} \tag{20}$$

$$L_2 = 20\log_{10} N_2 \tag{21}$$

where

$$20\log_{10} N_{\mathrm{n}} = -0.5 + 35\log_{10}\zeta_{\mathrm{n}} + 10\log_{10} F_{\mathrm{s}} \quad (22)$$

$$\zeta_{\mathrm{n}} = \frac{\frac{2\pi d_{\mathrm{n}}}{\lambda}}{\left(\frac{2\pi k_{\mathrm{e}} r_{\mathrm{e}}}{\lambda}\right)^{\frac{2}{3}}} \qquad \text{n=1,2,3} \quad (23)$$

and the $20\log_{10} F_{\mathrm{s}}$ is approximated from Fig. 13 in [12] by using a polynomial function expressed by:

$$20\log_{10} F_{\mathrm{s}} = -0.048{\zeta_{\mathrm{n}}}^3 + 1.0875{\zeta_{\mathrm{n}}}^2 + 4.0782\zeta_{\mathrm{n}} - 0.8806 \quad (24)$$

The L_3 is calculated by using the following polynomial function, which is obtained by fitting from Fig. 13 in [12].

$$L_3 = 0.0086{\zeta_3}^3 + 0.2063{\zeta_3}^2 + 11.0997\zeta_3 - 0.8934 \quad (25)$$

It needs to be mentioned that the total TX-RX distance d can be shorter than d_1+d_2, when the LOS is beyond the horizon. In this case, the d_3 is considered to be 'mathematically' negative with a corresponding 'positive' diffraction loss L_3 behaving as a 'gain'. The obtained total diffraction loss L with a function of the TX-RX distance d is shown in Fig 7, where $D_0 = d_1 + d_2 = 24.4$ km. The d_3 is considered to be negative with a 'gain-behaved' diffraction loss L_3, when $d < D_0$. It can be found that the total diffraction loss L can be positive, when d is short enough, resulting in $|L_3| > |L_1| + |L_2|$. L is set to zero, if the 'gain-behaved' L_3 is not less than $|L_1| + |L_2|$. The TX-RX distance (7.8026 km in Fig 7) for $L = L_1 + L_2 + L_3 = 0$ coincides with the path length of a clearance of 0.6 FFZ D_{06} mentioned in [4] and obtained by using:

$$D_{06} = \frac{D_{\mathrm{f}} \cdot D_{\mathrm{h}}}{D_{\mathrm{f}} + D_{\mathrm{h}}} \quad km \quad (26)$$

$$\text{frequency-dependent term}: \quad D_{\mathrm{f}} = 0.000389 f h_1 h_2 \quad (27)$$

$$\text{asymptotic term}: \quad D_{\mathrm{h}} = 4.1(\sqrt{h_1} + \sqrt{h_2}) \quad (28)$$

Here, f represents frequency in MHz. To summarize, the total diffraction loss in dB for both the LOS and the reflection path can be obtained by:

$$L = \begin{cases} L_1 + L_2 - |L_3| & \text{if } d \geq d_1 + d_2 \\ L_1 + L_2 + |L_3| & \text{if } D_{06} < d < d_1 + d_2 \\ 0 & \text{if } d < D_{06} \end{cases} \quad (29)$$

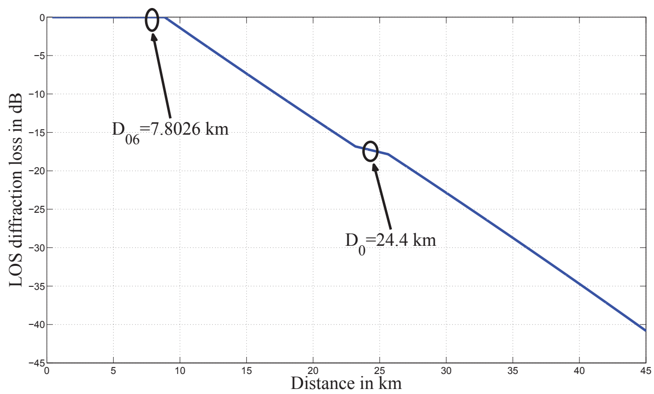

Fig. 7. Los diffraction loss for $h_1 = 14.1$ m, $h_2 = 9.5$ m, as a function of distance.

TABLE I
THE PARAMETER VALUES

Parameters	Values
RX antenna height for ant1	11.2 m
RX antenna height for ant2	14.1 m
TX antenna height	9.5 m
β_0	0.008
σ_h	0.25
k_e	1

E. Round Earth Loss Model

All the propagation effects listed in the equation (10) have been investigated in detail in the previous paragraphs. The diffraction effect is considered to influence both the LOS and the reflected ray, even though the reflected ray will be completely eliminated beyond a TX-RX distance of D_0. By including these effects in the two-ray geometrical model shown in Fig. 1, the model in (1) has been improved to:

$$P_{\mathrm{loss}} = 20\log_{10}\left(\frac{\lambda}{4\pi D_{\mathrm{los}}}\right) + 20\log_{10}(\eta) + L \quad (30)$$

$$\eta = |1 + S_{\mathrm{fun}} \cdot D \cdot R_{\mathrm{rough}} \cdot exp(jkD_{\mathrm{diff}})| \quad (31)$$

IV. Comparison with Measurements

A long-distance channel measurement campaign with a maximum distance of 45 km was performed in Trondheimsfjorden,Norway. The detailed description and corresponding analysis on the measurement data are given in [13]. The different path-loss models including the Round Earth Loss (REL) model, have been compared with the long-distance measurement in Fig. 8 and the corresponding parameter values are listed in Table I. The mean-square surface slope β_0 and the standard deviation of surface height distribution σ_{h} are set to small values due to small wave roughness under the stable weather condition during the long-distance measurement campaign. It can be found in Fig. 8 that the ITU model

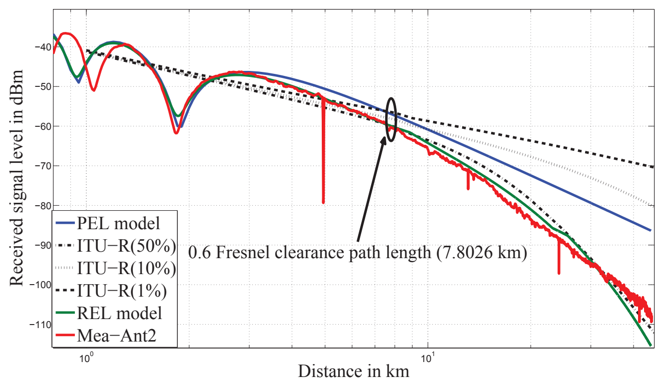

Fig. 8. Comparison between the REL mode, the PEL model, ITU-R model and the long-distance measurement.

doesn't include the fading dips (> 10 dB) at short TX-RX distances which are shown in the measurement results for the open sea environment and which are predicted by the PEL and REL model. On the other hand, the standard PEL model, which can't take the sea surface roughness, divergence and diffraction loss under different weather conditions into consideration, is unsuitable especially beyond D_{06}. Finally, the REL model matches the measurement result best with acceptable complexity and hight adaptivity.

V. Evaluation of the Model Parameters

We finally analyze the impact of various model parameters on the model predictions. The comparisons of a (vertically polarized) REL model with different β_0 and σ_h (the rest of parameter values are the same as in Table I) are displayed in Fig. 9 and Fig. 10, respectively. The larger β_0 and σ_h result in the decreased power of reflection path and the fading dips at short TX-RX become shallower. As it can be seen that the variations on RSL caused by using different β_0 and σ_h are reduced to zero when $d \geq D_{06}$. To conclude, the RSL obtained from the REL model is independent of with β_0 and σ_h when the TX-RX distance is beyond D_{06} and the shadowing and scattering effect will only influence the amplitudes of the fading dips within the distance of D_{06}.

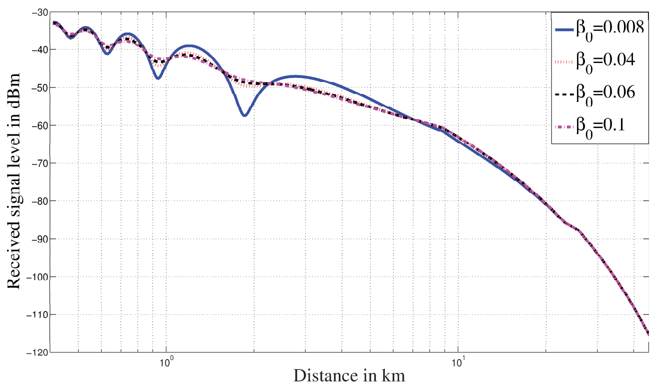

Fig. 9. REL with different mean-square surface slope β_0.

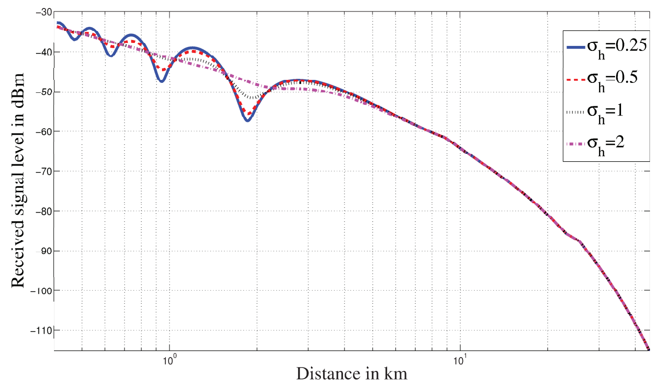

Fig. 10. REL with different standard deviation of surface height distribution σ_h.

VI. Conclusions

A deterministic path-loss model for the open-sea environment is presented based on the geometrical model of the round earth. With increasing TX-RX distance, the LOS ray will experience diffraction effects, while the reflection ray will be influenced by the scattering, divergence and diffraction effects. All these effects are described in detail, together with a theoretical analysis. The REL model has been validated by long-distance measurement results, and it fits the measurement very well. The REL model has been analyzed by using different channel parameters.

Acknowledgement

We want to thank the Ming Hsieh Department of Electrical Engineering of University of Southern California for hosting Kun Yang for a research visit during which part of this work was done. We also acknowledge Per Hjalmar Lehne at Telenor GBDR for his support with the channel sounder equipment that Telenor so kindly lent us. Further the practical support by Terje Mathiesen, NTNU and Karsten Husby, Odd Trandem and Torgrim Gjelsvik from Sintef ICT, is highly appreciated for the practical part of the measurements that has been successfully performed. The measurements has been funded by the Norwegian Research Council through the MARCOM project conducted by Fritz Bekkadal and Kay Fjørtoft at Sintef Marintek, Trondheim, Norway.

References

[1] N. H. Lu, "Linearized, Unified Two-Ray Formulation for Prapagation over a Plane Earth ," *proc. Sensor for Industry Conference, 2005. SIcon05*, Feb, 2005.
[2] J. Joe, S. K. Hazra, S. H. Toh, W. M. Tan, J. Shankar "Path Loss Measurements in Sea Port for WiMAX," *proc. IEEE Conference on Wireless Communications and Networking Conference, IEEE WCNC 2007*, 2007.
[3] S. R. Saunders and A. Aragon-zavala, *Antennas and Propagation for Wireless Communication Systems*. . John Wiley & Sons, 2007.
[4] ITU-R Recommendation P.1546-2, "Method for point-toarea predictions for terrestrial services in the frequency range 30 MHz to 3000 MHz," Sep. 2005.
[5] K. Yang, T. Ekman, T. Røste, and F. Bekkadal "A quasi-deterministic path loss propagation model for the open sea environment," in *IThe 14th International Symposium on Wireless Personal Multimedia Communications, 2011. WPMC11*. Brest, France, Oct. 2011.
[6] A. F. Molisch, *Wirless Communications 2nd edition*. . IEEE Press - Wiley, 2011.
[7] Kahma, K., D. Hauser, H.E. Krogstad, S. Lehner, J.A.J. Monbaliu, L.R. Wyatt "Measuring and Analysing the Directional Spectra of Ocean Waves," *EU COST Action 714, EUR 21367*, 465 p., ISBN 92-898-0003-8. 2005.
[8] J. D. Parsons, *The Mobile Radio Propagation Channel*. . John Wiley & Sons, 2000.
[9] B. J. Smith, "Geometrical Shadowing of a RandomRough Surface," *IEEE Transaction on antenna and propagation*, VOL. AP-15, NO. 5, Sep 1967.
[10] Y. Karasawa and T. Shiokawa "Characteristics of L-Band Multipath Fading due to Sea Surface Reflection," *IEEE Transaction on antenna and propagation*, VOL. AP-32, NO. 6, June 1984.
[11] K. A. Norton "The calculation of ground-wave field intensities over a finitely-conducting spherical earth," *Proc. IRE, Dec. 1941.*
[12] K. Bullington "Radio propagation above 30 megacycles," *Proc. IRE, Oct. 1947.*
[13] K. Yang, T. Røste, F. Bekkadal, K. Husby and O. Trandem "Long-distance propagation measurements of mobile radi sea at 2 GHz," *IEEE VTC Spring*, San Francisco, US, Sep. 2011.